A NOVEL ITERATIVE IMAGE RESTORATION ALGORITHM USING NONSTATIONARY IMAGE PRIORS

Esteban Vera[a], Miguel Vega[b], Rafael Molina[c], and Aggelos K. Katsaggelos[d]

a) Dept. of Electrical and Computer Engineering, University of Arizona, Tucson, AZ 85721.
b) Dept. de Lenguajes y Sistemas Informáticos, Univ. de Granada, 18071 Granada, Spain.
c) Dept. Ciencias de la Computación e I. A., Univ. de Granada, 18071 Granada, Spain.
d) Dept. of Electrical Engineering and Comp. Sc., Northwestern University, Evanston, IL 60208-3118.
estebanvera@email.arizona.edu, mvega@ugr.es, rms@decsai.ugr.es, aggk@eecs.northwestern.edu

ABSTRACT

In this paper, we propose a novel algorithm for image restoration based on combining nonstationary edge-preserving priors. We develop a Bayesian modeling followed by an evidence analysis inference approach for deriving the foundations of the proposed iterative restoration algorithm. Simulation results over a variety of blurred and noisy standard test images indicate that the presented method outperforms current state-of-the-art image restoration algorithms. We finally present experimental results by digitally refocusing images captured with controlled defocus, successfully confirming the ability of the proposed restoration algorithm in recovering extra features and details, while still preserving edges.

1. INTRODUCTION

Imaging systems are affected by several degradation sources, leading to blurry and noisy images that are not necessarily a faithful representation of the desired targets. Therefore, and regardless of the employed modality, image restoration is a critical task for recovering useful imagery for a variety of applications such as remote sensing, surveillance, medical diagnosis, and astronomy [1].

Unfortunately, the restoration of blurred and noisy images is an ill-posed inverse problem, typically solved by constrained optimization yielding to iterative regularization methods [2]. Nonetheless, regularized image restoration needs to address two main issues: the choice of the regularization function and the regularization parameter, or Lagrange multiplier. On the other hand, the use of Bayesian methods for image restoration has emerged as an elegant way of imposing the regularization term by means of a prior distribution, with the additional ability of allowing the estimation of both the regularization parameter and noise variance. Although it has been successfully applied to smoothness promoting priors [3, 4], Bayesian modeling imposes restrictions on the choice of the prior function and its distribution, which sometimes lead to untractable inference problems. The variational Bayes approximation [5] has allowed the successful usage of non-stationary sparsity promoting priors within the Bayesian framework, such as Total Variation (TV) in [6], Gaussian scale mixtures in [7], and the product of student-t experts in [8, 9].

This work has been supported by the Spanish "Comisión Nacional de Ciencia y Tecnologia" under contract TIN2010-15237. This work was partially done while Esteban Vera was pursuing his Phd degree in Electrical Engineering at the University of Concepción in Chile.

In this paper we propose a new approach for the combination of nonstationary edge-preserving image priors, in a similar spirit of the prior model based on the product of experts proposed in [10], but this time without the need of modifying the observation model, neither the need of using or setting any weighting parameters. The inference procedure is now based on the evidence analysis, or type-II maximum likelihood, following the work for stationary Bayesian restoration in [3]. However, as the resulting iterative parameter estimation update algorithm is computationally intractable, we derive an approximated algorithm by applying the Jacobi approximation to the inverse covariance matrices, that can be implemented in the Fourier domain.

We provide simulations for testing the novel restoration algorithm and compare its performance with state-of-the-art Bayesian restoration algorithms. We also present results from a digital refocusing experiment for images with different out-of-focus levels. The numerical and subjective evaluation of the results confirms the extended capabilities of the proposed restoration method in recovering more appealing images with enhanced details.

The paper is organized as follows. Section 2 presents the Bayes modeling and introduces the proposed new prior for the image restoration problem. In Section 3, the inference procedure for the image and parameters estimation is derived. Implementation issues are addressed in Section 4, using the proposed approximation for the estimation of the parameters. Section 5 and 6 present the results obtained for the simulations and the digital refocusing experiment. Finally, conclusions are summarized in Section 7.

2. BAYESIAN MODELING

2.1. Observation Model

A typical linear model for image degradation considers that the observed image $\mathbf{y}$ in lexicographical order, is the result of the convolution of the original and unknown image $\mathbf{x}$ with a blurring kernel operator $\mathbf{H}$, plus some additive noise $\mathbf{n}$, that is:

$$\mathbf{y} = \mathbf{H}\mathbf{x} + \mathbf{n},$$

If the noise component $\mathbf{n}$ is assumed to follow a Gaussian distribution, then the pdf of the observation model is expressed as:

$$p(\mathbf{y}|\mathbf{x}, \beta) \propto \beta^{N/2} \exp\left\{-\frac{\beta}{2}\|\mathbf{y} - \mathbf{H}\mathbf{x}\|^2\right\},$$

with β the inverse of the noise variance, and N the total number of pixels in the image.

2.2. Prior Modeling

Inspired by the prominent results obtained when combining more than one single prior as in the case of the field of experts Markov random fields (MRF) used for image denoising in [11], or the sparse prior approach used for image deconvolution in [12], we continue down the path of [10], but following a different inference procedure without approximating the covariance matrix for the prior prematurely.

Therefore, as image prior we define a zero-mean multivariate Gaussian distribution that combines the constraints given by a set of L filters $\mathbf{C}_i$ as follows:

$$p(\mathbf{x}|\mathbf{a}_1,\ldots,\mathbf{a}_L) \propto \left|\sum_{i=1}^{L}\mathbf{C}_i^t\mathbf{A}_i\mathbf{C}_i\right|^{1/2}\exp\left\{-\frac{1}{2}\sum_{i=1}^{L}\|\mathbf{A}_i^{1/2}\mathbf{C}_i\mathbf{x}\|^2\right\}$$

where $\mathbf{A}_i$ is a $N\times N$ diagonal matrix containing the hyperparameters a_i^j associated with the inverse variance (precision) of the response of each corresponding filter operator $\mathbf{C}_i$ for any given pixel j. Thus, $\mathbf{A}_i = \mathrm{DIAG}(\mathbf{a}_i)$, and $\mathbf{a}_i = [a_i^1, a_i^2, \ldots, a_i^N]^t$.

The advantage of using the proposed prior modeling is twofold. First, we avoid the election of any specific sparsity promoting shape for the prior distribution, since it is inherited in the non-stationarity of the precision hyperparameters. And second, by choosing a Gaussian distribution we are able to seek a tractable inference mechanism. In addition, in contrast to the previous approach proposed in [8], we have not imposed any informative hyperprior distribution on the hyperparameters.

3. BAYESIAN INFERENCE

The joint probability is written as follows:

$$\begin{aligned}p(\mathbf{y},\mathbf{x},\beta,\mathbf{a}_1,\ldots,\mathbf{a}_L) &\propto p(\mathbf{y}|\mathbf{x},\beta)p(\mathbf{x}|\mathbf{a}_1,\ldots,\mathbf{a}_L)\\ &\propto \left|\sum_{i=1}^{L}\mathbf{C}_i^t\mathbf{A}_i\mathbf{C}_i\right|^{1/2}\beta^{N/2}\exp\left\{-\frac{1}{2}\sum_{i=1}^{L}\|\mathbf{A}_i^{1/2}\mathbf{C}_i\mathbf{x}\|^2\right\}\\ &\times\exp\left\{-\frac{\beta}{2}\|\mathbf{y}-\mathbf{H}\mathbf{x}\|^2\right\}\end{aligned}$$

We choose to perform the inference for the desired hyperparameters based on the evidence analysis, or type-II maximum likelihood, also used in image restoration using stationary priors in [3, 4]. Then, by marginalizing over $\mathbf{x}$ we have that:

$$\begin{aligned}\ln p(\mathbf{y}|\beta,\mathbf{a}_1,\ldots,\mathbf{a}_L,) =& \frac{1}{2}\ln\left|\sum_{i=1}^{L}\mathbf{C}_i^t\mathbf{A}_i\mathbf{C}_i\right| + \frac{N}{2}\ln\beta\\ &- \frac{1}{2}\sum_{i=1}^{L}\|\mathbf{A}_i^{1/2}\mathbf{C}_i\bar{\mathbf{x}}\|^2 - \frac{\beta}{2}\|\mathbf{y}-\mathbf{H}\bar{\mathbf{x}}\|^2\\ &- \frac{1}{2}\ln\left|\sum_{i=1}^{L}\mathbf{C}_i^t\mathbf{A}_i\mathbf{C}_i + \beta\mathbf{H}^t\mathbf{H}\right|.\end{aligned}$$

Now, by taking the derivative with respect to the hyperparameter a_i^j corresponding to the element j of the diagonal matrix $\mathbf{A}_i$, we have that:

$$\begin{aligned}\frac{\delta\ln p(\mathbf{y}|\beta,\mathbf{a}_1,\ldots,\mathbf{a}_L)}{\delta a_i^j} =& \frac{1}{2}(\mathrm{tr}[(\sum_{i=1}^{L}\mathbf{C}_i^t\mathbf{A}_i\mathbf{C}_i)^{-1}\mathbf{C}_i^t\mathbf{J}^{jj}\mathbf{C}_i]\\ &- \bar{\mathbf{x}}^t\mathbf{C}_i^t\mathbf{J}^{jj}\mathbf{C}_i\bar{\mathbf{x}} - \mathrm{tr}[(\sum_{i=1}^{L}\mathbf{C}_i^t\mathbf{A}_i\mathbf{C}_i + \beta\mathbf{H}^t\mathbf{H})^{-1}\mathbf{C}_i^t\mathbf{J}^{jj}\mathbf{C}_i]),\end{aligned} \tag{1}$$

where $\bar{\mathbf{x}}$ is the MAP estimate for the unknown image, obtained by solving the following expression:

$$\bar{\mathbf{x}} = \left(\sum_{i=1}^{L}\mathbf{C}_i^t\mathbf{A}_i\mathbf{C}_i + \beta\mathbf{H}^t\mathbf{H}\right)^{-1}\mathbf{H}^t\mathbf{y}, \tag{2}$$

and $\mathbf{J}^{ij}$ is the single-entry matrix which is zero everywhere except at the entry (i,j).

Now, by setting the derivative equal zero, and defining $\Sigma_P = \sum_{i=1}^{L}\mathbf{C}_i^t\mathbf{A}_i\mathbf{C}_i$ and $\Sigma_T = \sum_{i=1}^{L}\mathbf{C}_i^t\mathbf{A}_i\mathbf{C}_i + \beta\mathbf{H}^t\mathbf{H}$, Eq. 1 can be written as:

$$\mathrm{tr}[\Sigma_P^{-1}\mathbf{C}_i^t\mathbf{J}^{jj}\mathbf{C}_i] = \bar{\mathbf{x}}^t\mathbf{C}_i^t\mathbf{J}^{jj}\mathbf{C}_i\bar{\mathbf{x}} + \mathrm{tr}[\Sigma_T^{-1}\mathbf{C}_i^t\mathbf{J}^{jj}\mathbf{C}_i].$$

Then, by following a similar approach for updating the hyperparameters as in [3], we are finally able to derive the iterative formula for any of the hyperparameters a_i^j at iteration $(k+1)$ as follows:

$$a_i^{j\,(k+1)} = \frac{a_i^{j\,(k)}\mathrm{tr}[\Sigma_P^{-1}\mathbf{C}_i^t\mathbf{J}^{jj}\mathbf{C}_i]}{\bar{\mathbf{x}}^{t\,(k)}\mathbf{C}_i^t\mathbf{J}^{jj}\mathbf{C}_i\bar{\mathbf{x}}^{(k)} + \mathrm{tr}[\Sigma_T^{-1}\mathbf{C}_i^t\mathbf{J}^{jj}\mathbf{C}_i]}, \tag{3}$$

where $\bar{\mathbf{x}}^{(k)}$ is computed at each iteration k using Eq. 2 with the corresponding hyperparameter matrices $\mathbf{A}_i^{(k)}$ obtained from the previous iteration of Eq. 3.

4. IMPLEMENTATION

Unfortunately, the parameters update formula in Eq. 3 is not implementable as is, mostly due to the computation of the inverse of the covariance matrices, Σ_P^{-1} and Σ_T^{-1}, since they are extremely large, which is computationally challenging. Therefore, we tackle this problem by applying the Jacobi diagonal approximation to the covariance matrices, which leads to a straightforward inversion process.

Matrix $\mathbf{H}^t\mathbf{H}$ can be successfully approximated by a weighted identity matrix such as $\mathbf{H}^T\mathbf{H} \approx h^2\mathbf{I}$, where h is a constant equivalent to the energy of the blurring kernel. In the case of a uniform (boxcar) kernel, h is the value of any of the filter coefficients. Let us now examine the matrices $\mathbf{C}_i^t\mathbf{A}_i\mathbf{C}_i$. By closely inspecting their diagonal elements, we realize that they can be obtained by following a certain rule, which at the end is related to the associated filter $\mathbf{C}_i$. Therefore, if $\mathbf{b}_i = \mathrm{diag}(\mathbf{C}_i^t\mathbf{A}_i\mathbf{C}_i)$ is the vector that contains all the diagonal elements of each $\mathbf{C}_i^t\mathbf{A}_i\mathbf{C}_i$ matrix, then $\mathbf{b}_i = \mathbf{D}_i^t\mathbf{a}_i$, where each $\mathbf{D}_i$ is a filter related to each $\mathbf{C}_i$. For example, if $\mathbf{C}_i$ is the matrix for the first order horizontal difference filter [1 -1], then $\mathbf{D}_i$ is the matrix for the linear filter [1 1]. In this way we found a diagonal approximation that resembles the original diagonal elements of any of the matrices $\mathbf{C}_i^t\mathbf{A}_i\mathbf{C}_i$, and it has the advantage of allowing us to compute all the diagonal elements of the inverse of each covariance matrix at once.

Now, in order to both stabilize the estimation process and also to regularize the covariance matrix elements, we apply the following

approximation $\mathbf{C}_i^t \mathbf{J}^{jj} \mathbf{C}_i \approx \mathbf{C}_i^t \mathbf{S}^{jj} \mathbf{C}_i$, where $\mathbf{S}^{jj}$ is an extended selecting matrix that not only selects the j^{th}-element such as $\mathbf{J}^{jj}$, but also selects the corresponding 4-connected neighbors. Thus, for any filter i and pixel position j, notice that the proposed approximation introduces regularization on the a_i^j parameters by combining its estimation with the estimation of its corresponding a_i^l parameters of its four l neighbor pixels.

The applied approximations allow us to perform the computation of the different a_i^j hyperparameters in parallel, by stacking in vector form the different equations. Note that the combination of the trace operator along with the matrix S^{jj} is equivalent to a moving average filter. Thus for any given associated filter C_i and any approximated covariance $\hat{\Sigma^{-1}}$ we have:

$$\left[\mathrm{tr}[\hat{\Sigma^{-1}}\mathbf{C}_i^t\mathbf{S}^{11}\mathbf{C}_i], \ldots, \mathrm{tr}[\hat{\Sigma^{-1}}\mathbf{C}_i^t\mathbf{S}^{NN})\mathbf{C}_i]\right]^t \approx 2\mathbf{B}\,\mathrm{diag}(\hat{\Sigma^{-1}}),$$

where $\mathbf{B}$ is a 4-connected spatial moving average filter. Finally we arrive at the following iterative update formula for the hyperparameters, which can be efficiently implemented in the Fourier domain:

$$\mathbf{a}_i{}^{(k+1)} = \mathrm{diag}\left[\mathrm{DIAG}\left(2\mathbf{B}\,\mathrm{diag}(\Sigma_P^{(k)\,-1})\right)\right. \quad (4)$$
$$\left. \times\ \mathrm{DIAG}\left(\mathrm{diag}((\mathbf{C}_i\bar{\mathbf{x}}^{(k)})(\mathbf{C}_i\bar{\mathbf{x}}^{(k)})^t) + 2\mathbf{B}\,\mathrm{diag}(\Sigma_T^{(k)\,-1})\right)^{-1}\right],$$

where the inverse covariances are $\Sigma_P^{(k)} = \sum_{i=1}^{L} \mathrm{DIAG}(\mathbf{D}_i^t \mathbf{a}_i{}^{(k)})$ and $\Sigma_T^{(k)} = \sum_{i=1}^{L} \mathrm{DIAG}(\mathbf{D}_i^t \mathbf{a}_i{}^{(k)}) + \beta h^2 \mathbf{I}$.

5. SIMULATION RESULTS

We implemented the algorithm in Eq. 4 using two options: NF2 that uses only the first order difference filters $\mathbf{c}_1 = [1\ -1]$ and $\mathbf{c}_2 = [1\ -1]^t$, and NF4 that also adds the diagonal filters $\mathbf{c}_3$ and $\mathbf{c}_4$ defined as follows:

$$\mathbf{c}_3 = \begin{bmatrix} 1 & 0 \\ 0 & -1 \end{bmatrix}, \qquad \mathbf{c}_4 = \begin{bmatrix} 0 & 1 \\ -1 & 0 \end{bmatrix}. \quad (5)$$

We compared the restoration performance of both versions against implementations of the Bayesian Total Variation (BTV) approach [6], and the product of student's- t priors (BST) [8]. We tested the restoration algorithms in a set of four standard images: Cameraman (CAM, 256×256), Lena (LEN, 256×256), Shepp-Logan Phantom (PHA, 256×256) and Barbara (BAR, 512×512. The images were degraded by applying a 9×9 uniform blur as the point spread functions (PSF), plus the addition of Gaussian noise for achieving an equivalent blurred to signal-to-noise ratio (BSNR) of 40dB, 30dB or 20dB.

For all experiments, every algorithm received as inputs the blurred image, the blurring PSF kernel, and the noise variance $\sigma = 1/\beta$. In addition, the stopping criteria for the iterative update of the hyperparameters was either $\|\mathbf{x}^{(k)} - \mathbf{x}^{(k-1)}\| < 10^{-3}$, or up to 30 iterations, whichever was met first. Also, the CG iterative process for estimating the restored image (Eq. 2) was terminated using a threshold of 10^{-4} or a maximum of 1000 iterations. Finally, the performance for each restoration was measured in terms of the improvement in signal-to-noise ratio (ISNR), which is defined as $20\log_{10}(\|\mathbf{x} - \mathbf{y}\|/\|\mathbf{x} - \hat{\mathbf{x}}\|)$. The averaged results obtained for the restoration performance given five realizations of the noise are summarized in Table 1.

Analyzing the results in Table 1, we can verify that both NF2 and NF4 present an overall superior ISNR for almost all images and noise levels, except for the Phantom image for higher noise levels, where BST performs better. This is reasonable since BST enforces sparsity in a stronger way, which makes it more suitable for piecewise images. A similar situation occurs with other tested PSF shapes such as the Gaussian (not reported). Although NF2 clearly outperforms BTV, note that the addition of two extra prior filters in the case of NF4 allows to significant improve the performance for higher BSNR, outperforming BTV, and often BST, in more than 10%, leading to a considerable improvement of more than 1 dB in ISNR for both Cameraman and Lena for all noise levels.

Table 1. Comparative restoration performance results in ISNR (dB).

		Uniform Kernel (9×9)			
BSNR	Method	CAM	LEN	PHA	BAR
40 dB	BTV	8.60	8.51	17.74	3.22
	BST	8.80	8.13	19.02	3.16
	NF2	9.34	9.13	20.03	**3.74**
	NF4	**9.75**	**9.63**	**23.05**	3.65
30 dB	BTV	5.08	5.89	11.00	1.71
	BST	5.89	5.50	**12.51**	1.61
	NF2	6.38	6.40	10.44	**2.01**
	NF4	**6.61**	**6.86**	12.14	1.93
20 dB	BTV	2.42	3.59	5.52	1.15
	BST	3.18	2.65	**8.25**	0.73
	NF2	**3.85**	4.22	6.83	**1.35**
	NF4	3.70	**4.45**	7.84	1.33

When closely inspecting the images from the simulations (not shown due to space limitations), we notice that the restored images using NF4 are smoother and less piecewise-like than the BTV and BST versions. Overall, soft transitions and shadowing effects due to illumination are better recovered, as well as some textures. Nevertheless, even though some edges are better defined, we are able to notice the appearance of some artifacts near some of the edges at lower BSNR.

6. EXPERIMENTAL RESULTS

We designed an experiment for systematically defocusing a target picture, while also retrieving the respective PSF from an illuminated optical fiber. For that, we mounted in a standard optical table a QImaging RETIGA EXi Monochrome 12-Bit Cooled CCD camera attached to a Computar H6Z0812 8-48 mm F1.2 C-mount zoom lens. We placed the desired target pictures, taken from a magazine (Communication Arts Photography Annual 48), at a distance of 1 meter from the main lens. We set the lens by fixing the f-stop at 4, and the focal distance at 30mm. The idea was to allow a proper focusing at the chosen distance, with enough depth of field in order to assure a near spatial invariant optical transfer function (OTF) at the widest area as possible in the field of view (FOV). We balanced the lighting conditions and integration time for compensating for the small aperture. In addition, we mounted at the same target distance one end of an optical fiber just in the center of the FOV, illuminated at the other end by a Thorlabs OSL 1-EC halogen lamp fiber illuminator. In this way, we are able to interchange between the target image and the end of the optical fiber.

From all the experiments made using several defocus levels and different target images, we applied all the implemented algorithms as explained in the previous section. However, now we utilized the procedure formerly proposed in [13] for confidently estimating the noise precision parameter β, using it as an input to all the deconvolution methods. In addition, we provide the algorithms with the

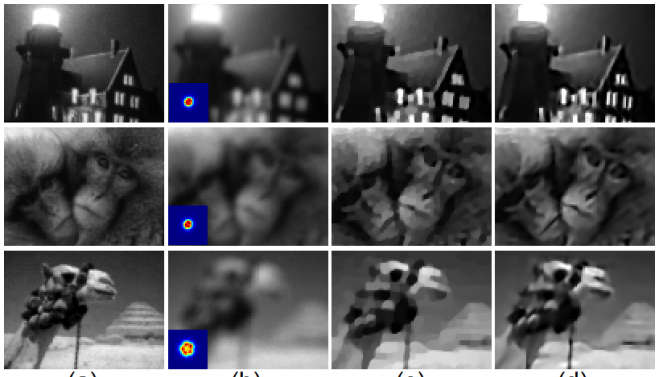

Fig. 1. Digital refocusing image samples. (a) Focused image; (b) Defocused image (Inset: measured PSF); (c) BTV restoration; (d) NF4 restoration.

retrieved normalized PSF for each target image. The experiment finally consisted of taking pictures of several image thumbnails of natural images. Each image was finally captured by a small area of the center of the CCD detector, leading to a resolution of 100×80 pixels each. Sample in-focus and out-of-focus images are displayed in Fig. 1(a) and Fig. 1(b), respectively.

Fig. 1 presents the restoration results from defocused images with medium (first two rows) and large size (third row) defocus, whose PSF support has a diameter of around 6 and 12 pixels, respectively (see inset in the blurred images of Fig. 1(b)), where we can notice a clear difference in terms of restoration quality between BTV in Fig. 1(c), and NF4 in Fig. 1(d). For instance, inspecting the first row we can check that NF4 was able to recover details from the windows of the house that are lost in BTV. Another feature, already visualized in the simulations, was that NF4 is able to recover smooth transitions of nontextured areas, such as the roof and the light source from the house image, the mouth of the mandrills, and also the nose and accessories of the camel, that have been lost when using BTV. In addition, NF4 generates restorations that have less of a piecewise appearance than those restored with BTV, producing more appealing natural images. Nonetheless, even though NF4 presents more pleasant restorations, some of the anticipated artifacts that arose in the simulations presented in Section 5 may be noticed near some edges.

7. CONCLUSION

In this paper, we proposed a new algorithm for image restoration based on combining many nonstationary edge-preserving priors. We developed a Bayesian modeling followed by an evidence analysis inference approach for deriving the parameters update algorithm, which was empirically approximated for tackling its computational difficulties mostly related to the inversion of large and ill-posed covariance matrices, also allowing a fast implementation. When comparing the restoration results of the proposed method with some of the latest state-of-the-art image restoration algorithms (BTV [6] and BST [8]) for a set of standard test images with simulated blurring and noise, we can conclude that in despite of some exceptions, specially the Phantom image with higher noise, the proposed algorithm outperformed the available methods in terms of ISNR and visual quality. The reported ISNR values indicate that the proposed algorithm surpasses by more than 10% the other methods, reaching a gap of more than 1 dB for the classic Cameraman and Lena test images for all noise levels. In addition, from the digital refocusing experiment performed for a variety of defocused natural images, the proposed algorithm clearly outperformed BTV in visual quality, recovering pleasant images plenty of details, while allowing realistic smooth transitions instead of pure piecewise solutions, which might be a desired feature when recovering natural images. Finally, it is foreseen that excellent results may be achieved by extending the proposed restoration algorithm for solving blind deconvolution and superresolution problems as well.

8. REFERENCES

[1] M.R. Banham and A.K. Katsaggelos, "Digital image restoration," *IEEE Signal Processing Magazine*, vol. 14, no. 2, pp. 24 –41, Mar 1997.

[2] A.K. Katsaggelos, S.D. Babacan, and Chun-Jen Tsai;, *Iterative Image Restoration*, chapter of The Essential Guide to Image Processing, Elsevier, 2009.

[3] R. Molina, "On the hierarchical bayesian approach to image restoration: applications to astronomical images," *IEEE Transactions on Pattern Analysis and Machine Intelligence*, vol. 16, no. 11, pp. 1122 –1128, Nov 1994.

[4] R. Molina, A.K. Katsaggelos, and J. Mateos, "Bayesian and regularization methods for hyperparameter estimation in image restoration," *IEEE Transactions on Image Processing*, vol. 8, no. 2, pp. 231 –246, Feb 1999.

[5] D.G. Tzikas, A.C. Likas, and N.P. Galatsanos, "The variational approximation for bayesian inference," *IEEE Signal Processing Magazine*, vol. 25, no. 6, pp. 131 –146, Nov 2008.

[6] S.D. Babacan, R. Molina, and A.K. Katsaggelos, "Parameter estimation in tv image restoration using variational distribution approximation," *IEEE Transactions on Image Processing*, vol. 17, no. 3, pp. 326 –339, Mar 2008.

[7] Rob Fergus, Barun Singh, Aaron Hertzmann, Sam T. Roweis, and William T. Freeman, "Removing camera shake from a single photograph," *ACM Trans. Graph.*, vol. 25, no. 3, pp. 787–794, 2006.

[8] G. Chantas, N. Galatsanos, A. Likas, and M. Saunders, "Variational bayesian image restoration based on a product of t - distributions image prior," *IEEE Transactions on Image Processing*, vol. 17, no. 10, pp. 1795 –1805, Oct 2008.

[9] G. Chantas, N.P. Galatsanos, R. Molina, and A.K. Katsaggelos, "Variational bayesian image restoration with a product of spatially weighted total variation image priors," *IEEE Transactions on Image Processing*, vol. 19, no. 2, pp. 351 –362, Feb 2010.

[10] G.K. Chantas, N.P. Galatsanos, and A.C. Likas, "Bayesian restoration using a new nonstationary edge-preserving image prior," *IEEE Transactions on Image Processing*, vol. 15, no. 10, pp. 2987 –2997, Oct 2006.

[11] Stefan Roth and Michael J. Black, "Fields of experts," *International Journal of Computer Vision*, vol. 82, no. 2, pp. 205–229, 2009.

[12] Anat Levin, Rob Fergus, Frédo Durand, and William T. Freeman, "Image and depth from a conventional camera with a coded aperture," *ACM Transactions on Graphics*, vol. 26, no. 3, pp. 70, 2007.

[13] R. Molina, J. Mateos, and A.K. Katsaggelos, "Blind deconvolution using a variational approach to parameter, image, and blur estimation," *IEEE Transactions on Image Processing*, vol. 15, no. 12, pp. 3715 –3727, Dec 2006.